Study on the χ Parameter for Compressible Diblock Copolymer Melts

Junhan Cho

Department of Polymer Science and Engineering, and Hyperstructured Organic Materials Research Center, Dankook University, San-8, Hannam-dong, Yongsan-gu, Seoul 140-714, Korea

Received January 14, 2002; Revised Manuscript Received April 19, 2002

ABSTRACT: A compressible random-phase approximation (cRPA) study is performed for a molten UCOT diblock copolymer of incompatible pairs to suggest an effective Flory-type interaction parameter χ_{cRPA} through mean-field spinodals. The compressible nature of a given copolymer system is carried by χ_{cRPA}, which is further divided into χ_{app} and χ_{comp}, where the former stands for the unfavorable exchange energy density and the latter contains the effects of compressibility difference between blocks. It is shown that χ_{app} and χ_{comp} upon pressurization contribute to phase stability in a reverse way to each other. The balance between those two χ's is found to yield the diversified behavior of microphase transitions under pressure for UCOT diblock copolymer melts. The comparison of the theory is made with the experimental phase behavior at different pressures for a typical UCOT system from polystyrene and polyisoprene. It is revealed that the microphase transitions and their response to pressure in the copolymer are mostly driven by χ_{app}. A Landau free energy combined with the cRPA in the case of $\chi_{comp} \approx 0$ is also suggested for the copolymer to yield a reasonable prediction of the pressure coefficients of the transition temperatures.

Introduction

Block copolymers from incompatible polymer pairs have been known to exhibit a microphase separation from a disordered state to an ordered state upon cooling, which is called the upper critical ordering transition (UCOT) behavior. The UCOT behavior is driven by the unfavorable interactions between dissimilar monomers comprising a given block copolymer. Ordered structures, which form nanoscale materials, are divided into classical and complex morphologies. The former includes body-centered cubic spheres (bcc), hexagonally packed cylinders (hex), and lamellar (lam) structures. Recently found morphologies such as bicontinuous gyroid and hexagonally perforated lamellar structures are categorized as the latter.[1−4]

In recent decades, there have been extensive theoretical developments to analyze the microphase separation behavior and transitions between equilibrium microstructures for block copolymers in a molten state or in solution.[4] Among them, Leibler suggested a Landau mean-field analysis based on the random-phase approximation (RPA) for weakly segregating diblock copolymer melts near spinodals.[5,6] It was revealed that asymmetric block copolymers undergo a general sequence of transitions from a disordered state to a metastable bcc, then to a hex, and then finally to a lam morphology upon cooling. A symmetric one was shown to exhibit a continuous transition from the disordered state to the lam morphology. Leibler's mean-field theory was later corrected by Fredrickson and Helfand to include concentration fluctuation effects.[7] It was shown that for a copolymer of finite molecular weight the continuous transition disappears and the direct transition to the hex or lam morphology is possible. While only the classical morphologies are treated in those theories, more advanced block copolymer theories have been developed in order to analyze complex morphologies.[4] Harmonic corrections to Leibler and Fredrickson−Helfand theories have been made to stabilize the gyroid between the hex and the lam morphologies.[4,8−14] All of the block copolymer theories just mentioned are based on the common assumption of system incompressibility.

There have emerged in the past decade a different class of theories that take finite compressibility into consideration in a given block copolymer system. Those theories are based on the so-called compressible RPA approaches. Freed and co-workers were the first to incorporate finite compressibility into the incompressible RPA by allowing for vacancy.[15−22] Other theories have also been formulated using vacancies as a pseudosolvent in the incompressible treatment.[23−25] Two-body correlation functions or spinodals from the compressible RPA theories were used to explain a newly found microphase separation behavior, which is induced inversely by heating and thus referred to as the lower critical ordering transition (LCOT). Some diblock copolymer melts from polystyrene (PS) and lower alkyl polymethacrylates exhibited such a LCOT behavior.[26−29] The existence of LCOT indeed neccessitates compressibility because it is considered to be driven by the difference in volume fluctuations between constituent polymers.

Meanwhile, a new compressible RPA theory was recently introduced by the present author.[30−33] The formulation of the theory is considered to be unique because Akcasu's general compressible RPA formalism,[34,35] which discards the Lagrange multiplier for the incompressibility constraint in RPA calculations, was used instead of the pseudosolvent technique. Finite compressibility was incorporated into the theory through effective RPA interaction fields, which is obtained from an off-lattice equation-of-state (EOS) model by Cho and Sanchez (CS) in Appendix A.[30,36] Intermonomer correlation functions and the corresponding vertex functions in the Landau expansion of the free energy in packing density fluctuations for diblock copolymer melts were formulated up to quartic order.[32,33] Compressible Landau free energy densities treating classical microphase morphologies were then obtained for the following two systems: one is for LCOT diblock copolymer melts that microphase separate upon heating due to compressibility difference between blocks;[32] the other is for UCOT copolymer melts with identical compressibility for both blocks, whose microphase separation is induced by the

10.1021/ma020059l CCC: $22.00
Published on Web 06/04/2002

unfavorable energetics.[33] The transition temperatures, equilibrium microphase morphologies, and the order of transition were discussed with the help of such Landau mean-field energies. It was found that the continuous transition for a symmetric copolymer vanishes in the LCOT case but is restored in the UCOT systems with identical compressibilities for both blocks. In all cases, the general sequence of microphase transition (disorder → bcc → hex → lam) was sustained as the segregation tendency strengthened.

One of the merits of our compressible RPA analysis is that pressure effects on microphase separation behavior can be predicted at least in a mean-field sense. Such calculations through the proper Landau free energy were performed for diblock copolymers from PS and polybutadiene (PBD), denoted as P(S-*b*-BD), which is a typical UCOT system.[33] It was found that the transition temperatures increase linearly with pressure, which was indeed harmonious with the small-angle scattering measurements for the same system by Stamm and co-workers[37] and by Schwahn and co-workers.[38] Though the present theory was successfully applied to the P(S-*b*-BD) melts, in particular the pressure effects on the transition temperatures for the copolymer, there have been completely different reports about the pressure effects on the transitions for other UCOT block copolymers. A slightly asymmetric diblock copolymer of poly(ethylene−propylene) and poly(ethyl ethylene), denoted as P(EP-*b*-EE), was shown to reveal a monotonically decreasing spinodal point upon pressurization up to 100 MPa.[39] Meanwhile, a symmetric diblock copolymer of poly(ethylene−propylene) and poly(dimethylsiloxane), denoted as P(EP-*b*-DMS), has shown the intermediate behavior: the order−disorder transition temperature first decreases upon pressurization up to ∼50 MPa, then increases after that.[40]

It is our desire to envision a theoretical basis of such a diversified behavior of microphase transitions for UCOT systems upon pressurization. In this study, mean-field spinodals from our compressible RPA theory are carefully examined to define an effective Flory-type χ_{cRPA} parameter for compressible diblock copolymers. The χ_{cRPA} parameter is to be divided into χ_{app} and χ_{comp}, where the former stands for the unfavorable energetics and the latter contains the effects of compressibility difference. To view the action of those two χ's on the phase behavior of UCOT systems, a commonly used block copolymer from PS and polyisoprene (PI), denoted as P(S-*b*-I), is chosen as a model system. The two χ's are analyzed with the help of molecular parameters, which is based on the CS EOS model, that characterize the constituents. It is found that χ_{app} and χ_{comp} are competing, so that the balance between the two can indeed give all the observed behavior of the pressure dependence of various transitions. The experimental small-angle X-ray scattering data of the order−disorder transition temperatures for P(S-*b*-I), measured by Hadjuk et al. with varying pressure,[41] are to be compared with the theoretically predicted behavior. The comparison between the theory and the experiments leads to a proper expression of the spinodals, which then yields a compressible Landau free energy for the copolymer to predict a complete mean-field phase diagram and the pressure dependence of the transition temperatures against composition.

Compressible RPA and Effective χ Parameter

It is our primary concern here to suggest an effective Flory type interaction parameter that drives microphase separation in compressible UCOT block copolymer systems. Spinodals or linear stability condition is to be examined to elicit such an interaction parameter. Let us begin with the system description. The system of interest consists of A−B diblock copolymers with r_1 monomers of A type and r_2 monomers of B type to have the overall size r_T ($=\sum_i r_i$). All the monomers in the system are assumed to have the identical diameter σ. The $\phi_1 \equiv r_1/r_T$ defines a volume fraction of A monomers on the copolymer chains. The ϕ_2 then indicates that of B monomers and thus $\phi_2 = 1 - \phi_1$.

The spinodals can be obtained from the Fourier transformed second-order correlation functions $S_{ij}(\vec{q})$ between *i*- and *j*-monomers, where the Fourier component $\vec{q}$ physically denotes the scattering vector. According to the RPA theory by Leibler in the incompressible situation,[6] there is only one independent correlation function because $S_{11} = S_{22} = -S_{12}$ due to the incompressibility constraint. Hence, the spinodals are given by the vanishing $1/S_{11}$ at a certain nonzero q ($\equiv|\vec{q}|$),[42] which can be written explicitly as

$$1/S_{11} = \left(\frac{\bar{S}_{11}^{\,0} + \bar{S}_{22}^{\,0} + 2\bar{S}_{12}^{\,0}}{\bar{D}}\right) - 2\chi_F \qquad (1)$$

where the term in the bracket implies the contribution from the correlation functions $\bar{S}_{ij}^{\,0}$ for noninteracting Gaussian chains, and $\bar{D}$ is the corresponding determinant as $\bar{D} = \det[\bar{S}_{ij}^{\,0}]$. The symbol χ_F denotes the Flory exchange energy from interactions between monomers in a given system.

With finite compressibility allowed, the same copolymer system requires all the three correlation functions, which are S_{11}, S_{22}, and S_{12}, to be independent. This procedure then invalidates the spinodal condition in eq 1 and the unambiguous definition of Flory χ_F. A proper substitute for χ_F is sought for to describe compressible nature in the system. The spinodals in this case are obtained when the determinant, $\det[S_{ij}^{-1}]$, of the inverses of those correlation functions vanishes at a positive q. The correlation functions S_{ij}'s are approximated in the compressible RPA theory by the present author to[30−33]

$$S_{ij} = [S_{ij}^{\,0\,-1} + \beta W_{ij}]^{-1} \qquad (2)$$

where $S_{ij}^{\,0}$ in eq 2 is also the Gaussian correlation function. However, in the compressible situation, $S_{ij}^{\,0}$ is given as $\eta\bar{S}_{ij}^{\,0}$, where η is the total packing density that is the fraction of volume occupied by all molecules but free space in the system. This modification results in the fact that contact probability between monomers is diluted by the presence of free volume. The βW_{ij} ($=L_{ij} - \beta\epsilon_{ij}^{app}$), where β is $1/kT$ as usual, indicates the interaction fields that contain the excluded volume contribution (L_{ij}) and nonbonded interaction contribution ($\beta\epsilon_{ij}^{app}$). Finite compressibility is indeed incorporated into RPA through the interaction field W_{ij}. The L_{ij} and ϵ_{ij}^{app} are well-defined in Appendix B. Using

those S_{ij}'s can yield the mathematical expression of the determinant. The determinant $\det[S_{ij}^{-1}]$ is now forced to be written as

$$\det[S_{ij}^{-1}] = L_{11}\left(\frac{S_{11}^{0} + S_{22}^{0} + 2S_{12}^{0}}{D}\right) - L_{11}\frac{2\chi_{\mathrm{cRPA}}}{\eta} \quad (3)$$

where D is equal to $\det[S_{ij}^{0}]$. In eq 3, we have introduced χ_{cRPA} as the desired effective interaction parameter in the compressible case.[43] The χ_{cRPA} is further defined to be divided into two terms as

$$\chi_{\mathrm{cRPA}} = \chi_{\mathrm{app}} + \chi_{\mathrm{comp}} \quad (4)$$

where the requisite definitions of the two χ's in eq 4 are as follows.

The χ_{app} is dependent on energetic terms $\beta\epsilon_{ij}^{\mathrm{app}}$, and defined as

$$\frac{\chi_{\mathrm{app}}}{\eta} = \frac{1}{2}(\beta\epsilon_{11}^{\mathrm{app}} + \beta\epsilon_{22}^{\mathrm{app}} - 2\beta\epsilon_{12}^{\mathrm{app}}) \quad (5)$$

The $\beta\epsilon_{ij}^{\mathrm{app}}$ involves a complicated functional form, as can be seen in eq B8. However, the desired sum in eq 5 is greatly simplified to

$$\chi_{\mathrm{app}} = \frac{1}{2}f_{\mathrm{p}}\chi|u(\eta)| \quad (6)$$

where f_{p} is simply 4 and $u(\eta)$, given in eq A2, describes the dependence of the nonbonded interactions on the packing density η. In eq 6, χ is the familiar exchange energy as $\chi = (\bar{\epsilon}_{11} + \bar{\epsilon}_{22} - 2\bar{\epsilon}_{12})/kT$, where a self ($\bar{\epsilon}_{ii}$) and a cross interaction parameter ($\bar{\epsilon}_{ij}$) represent the potential depth of the conventional Lennard-Jones (L-J) interactions for AA or BB contacts and for AB contacts, respectively. It was shown in our previous communication that $|u(\eta)|$ is linearly increasing with η in the useful η range.[33] It can then be said that χ_{app} implies the exchange energy density.

The following χ_{comp} is dependent not only on $\beta\epsilon_{ij}^{\mathrm{app}}$ but also on L_{ij} and S_{ij}^{0}:

$$\begin{aligned}\frac{\chi_{\mathrm{comp}}}{\eta} = &-\frac{1}{2L_{11}}\{\beta\epsilon_{11}^{\mathrm{app}}\beta\epsilon_{22}^{\mathrm{app}} - (\beta\epsilon_{12}^{\mathrm{app}})^2\} + \\ &\frac{1}{2L_{11}}\{(-L_{11} + L_{22})\beta\epsilon_{11}^{\mathrm{app}} - 2(-L_{11} + L_{12})\beta\epsilon_{12}^{\mathrm{app}}\} - \\ &\frac{1}{2L_{11}}\left\{\frac{S_{11}^{0}}{D}(-\beta\epsilon_{11}^{\mathrm{app}}) + \frac{S_{22}^{0}}{D}(-L_{11} + L_{22} - \beta\epsilon_{22}^{\mathrm{app}}) + \right. \\ &\left.\frac{2S_{12}^{0}}{D}(-L_{11} + L_{12} - \beta\epsilon_{12}^{\mathrm{app}})\right\} - \\ &\frac{1}{2L_{11}}\left(\frac{1}{D} + L_{11}L_{22} - L_{12}^{2}\right) \quad (7)\end{aligned}$$

It can be further shown that the term in the first bracket of eq 7 is rewritten as

$$\begin{aligned}\beta\epsilon_{11}^{\mathrm{app}}\beta\epsilon_{22}^{\mathrm{app}} - (\beta\epsilon_{12}^{\mathrm{app}})^2 = &f_{\mathrm{p}}^{2}[\beta\bar{\epsilon}_{11}\beta\bar{\epsilon}_{22} - \\ &(\beta\bar{\epsilon}_{12})^2]\left\{\left(\frac{u(\eta)}{\eta}\right)^2 + 2u(\eta)\frac{\partial}{\partial\eta}\left(\frac{u(\eta)}{\eta}\right)\right\} - \frac{f_{\mathrm{p}}^{2}}{4}\eta^2[\beta\bar{\epsilon}_{11} - \\ &\beta\bar{\epsilon}_{22} - \chi(1 - 2\phi_1)]^2\left\{\frac{\partial}{\partial\eta}\left(\frac{u(\eta)}{\eta}\right)\right\}^2 + f_{\mathrm{p}}^{2}[\beta\bar{\epsilon}_{11} + \beta\bar{\epsilon}_{22} - \\ &2\beta\bar{\epsilon}_{12}]\frac{u(\eta)}{\eta}\frac{1}{2}\sum_{k,l}\eta_k\eta_l\beta\bar{\epsilon}_{kl}\frac{\partial^2}{\partial\eta^2}\left(\frac{u(\eta)}{\eta}\right) \quad (8)\end{aligned}$$

It is seen from eq 7 that χ_{comp} is additionally dependent on the scattering vector due to $S_{ij}^{0}(\vec{q})$. The χ_{comp} is mathematically involved, as can be seen from eqs 7 and 8. However, it will be shown later that χ_{comp} is dependent on the compressibility difference between the constituent blocks. The competition between χ_{app} and χ_{comp} is to yield various pressure dependence of microphase transition temperatures.

The well-known behavior of the incompressible diblock copolymers shown in eq 1 can be retrieved in a formal way from the compressible RPA. The correlation function S_{11} between two A monomers can now be written as

$$S_{11} = \frac{S_{22}^{-1}}{\det[S_{ij}^{-1}]} = \frac{1 + (S_{22}^{0\,-1} - L_{11} + L_{22} - \beta\epsilon_{22}^{\mathrm{app}})/L_{11}}{\left(\frac{S_{11}^{0} + S_{22}^{0} + 2S_{12}^{0}}{D}\right) - 2\frac{\chi_{\mathrm{app}} + \chi_{\mathrm{comp}}}{\eta}} \quad (9)$$

As the system becomes incompressible ($\eta \rightarrow 1$), L_{ij} goes to infinity. The χ_{comp} then vanishes because all the terms in eq 7 are divided by L_{11}. As the numerator in eq 9 also converges to 1, the resultant equation for S_{11} is essentially reduced to eq 1 for the incompressible diblock copolymers.

Compressibility Difference between Blocks

In this section, it is to be investigated how the compressibility difference between blocks affects χ_{app} and χ_{comp} and, thus, the phase behavior of UCOT diblock copolymer melts. As was mentioned in the Introduction, P(S-*b*-I), which is a typical UCOT system, is chosen here as a model system for our purpose. To characterize the molten P(S-*b*-I), one needs various molecular parameters based on the CS model in Appendix A. Those parameters include the self-interaction parameter $\bar{\epsilon}_{ii}$, the monomer diameter σ_i, and the chain size r_i for either PS or PI and, finally, the parameter $\bar{\epsilon}_{ij}$ for cross interactions between PS and PI. The present analysis deals only with the case that all the σ_i's are identical for simplification purposes. The discrepancy in monomer sizes, if involved, is resolved by employing the average monomer diameter, $\sigma = (\sigma_1 + \sigma_2)/2$, for both polymers.

In Table 1, the requisite molecular parameters for the two constituents, PS and PI, are tabulated. It is seen in this table that a combined parameter, $r_i\pi\sigma_i^3/6\mathrm{MW}_i$, where MW is the molecular weight of a given constituent polymer, is presented instead of the chain size r_i. The r_i can be obtained from setting proper molecular weights. The subscripts 1 and 2 hereafter indicate PS and PI, respectively. The parameters for PS, with the

Table 1. Molecular Parameter Sets for PS and PI Used in This Study

parameters	PS[a]	PI[b]		
σ (Å)	4.04	4.04	4.08	4.35
$\bar{\epsilon}/k$ (K)	4107.0	3678.6	3727.6	4057.7
$r\pi\sigma^3$/6MW (cm^3/g)	0.418 57	0.491 55	0.493 00	0.502 09

[a] The molecular parameters for PS are those employed in our previous work, where its volume data are obtained from refs 44 and 45. [b] The molecular parameter sets for PI are determined from fitting its volume data in refs 45 and 46 to eq A3 with the indicated σ_{PI}'s. The molecular parameters associated with $\sigma_{PI} = 4.04$ Å give the least average error in estimating the volume of pure PI in the experimental temperature−pressure range. The average error gradually increases, as σ_{PI} deviates from 4.04 Å. [c] The experimental volume data of pure PS are only smaller by ∼1% than those of pure PI in the temperature range from 383 to 473 K at 0.1 MPa. Such volume differences are increased to ∼4% in the same temperature range at 100 MPa.

Table 2. Ratio of $\bar{\epsilon}_{12}$ to $(\bar{\epsilon}_{11}\bar{\epsilon}_{22})^{1/2}$ for the PS/PI System Associated with the Various Choices of σ_{PI}'s

σ_{PI} (Å)	$\bar{\epsilon}_{12}/(\bar{\epsilon}_{11}\bar{\epsilon}_{22})^{1/2}$
4.04	0.997600
4.08	0.997080
4.35	0.995337

monomer size $\sigma_1 = 4.04$ Å, were obtained from those employed in our previous communications.[30,44,45] In the case of PI, we prepared several sets of its molecular parameters based on the CS model by fitting its volumetric data[45,46] with the various choices of monomer size σ_2 from 4.04 to 4.35 Å. This procedure enables us to deliberately control the compressibility difference between PS and PI in their mixture. Using the molecular parameters associated with $\sigma_2 = 4.35$ Å, the differences in the calculated volume between the two polymers are kept less than 1% over 100 MPa. The compressibility difference between the two thus becomes minimal, which is caused by that the self-interaction parameters $\bar{\epsilon}_{ii}$'s for both polymers are similar to each other in this situation. As σ_2 is decreased, the compressibility difference is gradually increased along with the decreasing $\bar{\epsilon}_{22}$. The differences in the calculated volume between PS and PI in the case of $\sigma_2 = 4.04$ Å become on the order of 1.5−2.5% over 100 MPa in the same temperature range as before. However, it will be shown in a later part of this section that those with $\sigma_2 = 4.35$ Å give better results in describing the pressure effects on the phase behavior.

In analyzing the phase behavior of the copolymer, a proper choice of the cross-interaction parameter $\bar{\epsilon}_{12}$ is essential. $\bar{\epsilon}_{12}$ is determined by adjusting it around the geometric mean $(\bar{\epsilon}_{11}\bar{\epsilon}_{22})^{1/2}$ of self-interaction parameters to predict a correct critical temperature using eq A4 in Appendix A for the corresponding low molecular weight PS/PI blends measured by Rudolf and Cantow.[47] Each molecular parameter set for PI in Table 1 demands its own $\bar{\epsilon}_{12}$ to predict the reported critical temperature. It is shown that the different sets of parameters yield comparable predictions of the phase diagram with the adjusted $\bar{\epsilon}_{12}$'s despite of the differences in estimating volumetric properties for this PS/PI system. In Table 2, such $\bar{\epsilon}_{12}$'s associated with σ_2's for PI are tabulated.

Mean-field spinodal points in compressible block copolymer systems are given by the vanishing $\det[S_{ij}^{-1}]$ at a certain $q > 0$. Figure 1 depicts the plot of $\det[S_{ij}^{-1}]$ against the squared wavenumber $q^2R_G^2$ for the P(S-*b*-I) melt with the MW's of 5100 and 15 400 for PS and PI blocks, respectively. The R_G denotes the gyration radius

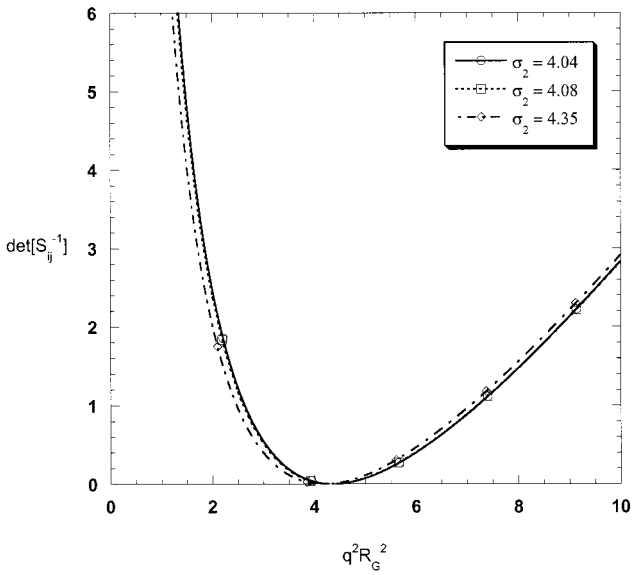

Figure 1. $\det[S_{ij}^{-1}]$ at a certain temperature plotted as a function of the squared dimensionless wavenumber $q^2R_G^2$ for the P(S-*b*-I) melt of the total MW = 20 500 with the MW of PS block being of 5100. The R_G is the gyration radius of chains in the system. The molecular parameter sets for PI to construct the plots correspond to the indicated σ_{PI}'s. The characteristic $q^{*2}R_G^2$, at which $\det[S_{ij}^{-1}]$ possesses a minimum, is found to be 4.357, 4.337, and 4.199 for $\sigma_{PI} = 4.04$, 4.08, and 4.35 Å, respectively. The vanishing minima of $\det[S_{ij}^{-1}]$ imply that the plots are generated at spinodal temperatures.

of chains. As seen in this figure, the copolymer experiences a minimum of $\det[S_{ij}^{-1}]$ at $q = q^*$, where $q^{*2}R_G^2 \sim 4$ at the given composition. At this q^*, $\det[S_{ij}^{-1}]$ vanishes, which indicates that Figure 1 is indeed generated at the spinodal temperature T_s. There are three such lines of $\det[S_{ij}^{-1}]$ in Figure 1, where each one is constructed by using the molecular parameter set associated with the indicated σ_2.

The newly defined χ_{cRPA} is divided into χ_{app} and χ_{comp}. It was already mentioned that χ_{app} represents the unfavorable exchange energy density to give block copolymers UCOT character. The remaining part of χ_{cRPA}, i.e., χ_{comp}, however, is not well described yet. As seen in eqs 7 and 8, χ_{comp} is a complicated function of composition, temperature, density, and even scattering vector $\vec{q}$. Various molecular parameters are also explicitly involved in this χ_{comp}. To elucidate the behavior of χ_{comp}, it is evaluated at T_s for the copolymer with the same composition as in Figure 1, as q is increased. Figure 2 shows the plot of χ_{comp} again as a function of the squared wavenumber $q^2R_G^2$ instead of q. It is seen in this figure that χ_{comp} varies rather strongly with q and possesses a maximum at $q = q^*$, at which $\det[S_{ij}^{-1}]$ has a minimum. In Figure 2, the effects of the molecular parameters for PI on the behavior of χ_{comp} are also shown. It is observed that χ_{comp} at $q = q^*$, associated with $\sigma_2 = 4.35$ Å, almost vanishes, whereas those with $\sigma_2 = 4.04$ and 4.08 Å are sizable. As σ_2 departs from 4.35 Å, the compressibility difference between PS and PI increases. Therefore, it can be said that χ_{comp} contains the effects of compressibility difference between the two blocks.[48]

Tables 3−5 show the comparison of χ_{app} and χ_{comp} using the molecular parameter sets with the three selected σ_2's for the copolymer with the same composition as in Figures 1 and 2. Those two χ's are first evaluated at 0.1 MPa and at T_s, and then subsequently

Table 3. Comparison of All the χ's for P(S-*b*-I)[a] with σ_{PI} = 4.04 Å, Evaluated at 329.96 K (T_s at 0.1 MPa) and at Elevated Pressures

pressure (MPa)	$2\chi_{app}$	$2\chi_{comp}$[b]	$2\chi_{cRPA}$
0.1	0.082564	0.009608	0.092172[c]
20	0.083492 (0.083876)	0.008194 (0.008296)	0.091686 (0.092172)
40	0.084318 (0.084959	0.007016 (0.007212)	0.091334 (0.092172)
60	0.085056 (0.085867)	0.006028 (0.006304)	0.091084 (0.092172)
80	0.085719 (0.086638)	0.005192 (0.005533)	0.090912 (0.092172)
100	0.086319 (0.087300)	0.004481 (0.004871)	0.090799 (0.092172)

[a] P(S-*b*-I) with the MW's of 5100 and 15 400 for PS and PI blocks, respectively. [b] χ_{comp} is only evaluated at $q = q^*$. [c] This value is indeed the Gaussian contribution to spinodals, which is $\eta(S_{11}° + S_{22}° + 2S_{12}°)/2D$ calculated at $q = q^*$. [d] For comparison purposes, χ's at the indicated pressures (>0.1 MPa) and at the corresponding T_s's are also given inside the brackets.

Table 4. Comparison of All the χ's for P(S-*b*-I)[a] with σ_{PI} = 4.08 Å, Evaluated at 339.29 K (T_s at 0.1 MPa) and at Elevated Pressures

pressure (MPa)	$2\chi_{app}$	$2\chi_{comp}$[b]	$2\chi_{cRPA}$
0.1	0.084229	0.007228	0.091457[c]
20	0.085201(0.085216)	0.006237 (0.006241)	0.091439 (0.091457)
40	0.086066 (0.086030)	0.005438 (0.005427)	0.091504 (0.091457)
60	0.086838 (0.086711)	0.004789 (0.004747)	0.091627 (0.091457)
80	0.087531 (0.087288)	0.004259 (0.004170)	0.091789 (0.091457)
100	0.088157 (0.087782)	0.003822 (0.003675)	0.091979 (0.091457)

[a] P(S-*b*-I) has the same composition as in Table 3. [b] χ_{comp} is only evaluated at $q = q^*$. [c] This $2\chi_{cRPA}$ at spinodals or, equivalently, the Gaussian contribution to spinodals is slightly different from that in Table 3, which is caused by the differences in the rescaled chain sizes according to the indicated σ_{PI}'s. [d] For comparison purposes, χ's at the indicated pressures (>0.1 MPa) and at the corresponding T_s's are given inside the brackets as before.

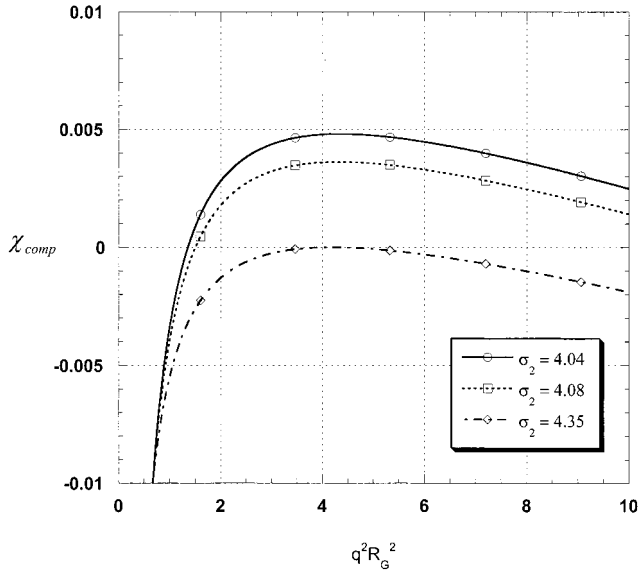

Figure 2. χ_{comp} plotted against $q^2R_G^2$ for the P(S-*b*-I) with MW = 20 500 at the same composition as in Figure 1. Using the molecular parameter sets for PI corresponding to the indicated σ_{PI}'s, the χ_{comp} is evaluated at the spinodal temperatures.

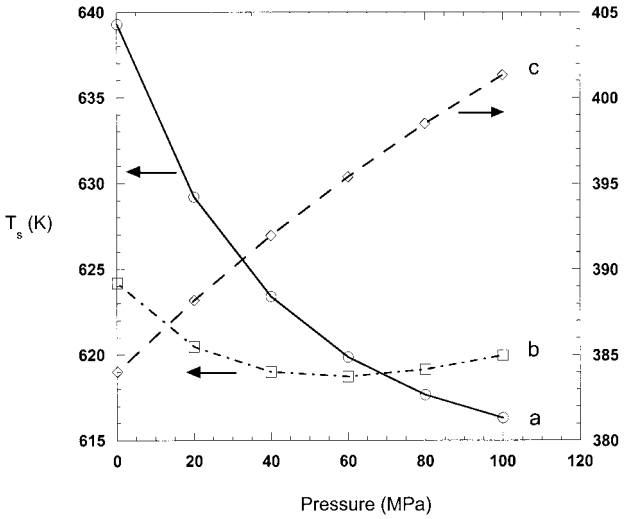

Figure 3. Calculated spinodal temperatures T_S plotted as a function of pressure for the P(S-*b*-I) melt of the total MW = 20 500 with the MW of PS block being either 10 000 (a,b) or of 5100 (c). The σ_{PI}'s of 4.04, 4.08, and 4.35 Å are respectively used to yield plots a−c.

at higher pressures while temperature is fixed. For comparison purposes, the χ's at the indicated pressures and at the corresponding T_s's are also given in these tables. The $\vec{q}$-dependent χ_{comp} is calculated only at $q = q^*$. In this UCOT system, χ_{app} is in all cases far greater than χ_{comp}, which indicates that the microphase separation is largely driven by the unfavorable energetics χ_{app}. The ratio of χ_{comp} to χ_{app} is, however, shown to increase in accordance with the compressibility difference between PS and PI. As χ_{app} and χ_{comp} differ from each other in their meaning, applying pressure yields different responses from the two χ's. It is easily conceived that applied pressure in general suppresses the compressibility difference between the blocks. Such an action is shown to favor mixing because χ_{comp} is also suppressed by pressurization. This situation is apparent in Tables 3 and 4 in the cases of σ_2 = 4.04 and 4.08 Å, respectively, where the compressibility difference is appreciable. Even in the case of σ_2 = 4.35 Å, it is seen in Table 5 that χ_{comp} at the spinodal points, though only minute, is still suppressed by the applied pressure.[49] The χ_{app} responds in an opposite direction: χ_{app} tends to increase with pressure due to the increased density η. The increased χ_{app} then hampers miscibility. These results are well demonstrated in Tables 3−5. It can then be easily seen that those two χ's are competing.

The spinodals for the P(S-*b*-I) melt at different compositions are plotted as a function of pressure up to 100 MPa in Figure 3, as each line (a−c) therein is obtained for the molecular parameter set of PI corresponding to the indicated σ_2. It is seen in this figure that the spinodals in the case of σ_2 = 4.04 Å are apparently decreasing with pressure.[50] This result can be understood from Table 3 because χ_{comp} acts an important role in χ_{cRPA}. Pressure significantly reduces

Table 5. Comparison of All the χ's for P(S-*b*-I)[a] with σ_{PI} = 4.35 Å, Evaluated at 384.00 K (T_s at 0.1 MPa) and at Elevated Pressures

pressure (MPa)	$2\chi_{app}$	$2\chi_{comp}$[b]	$2\chi_{cRPA}$
0.1	0.087811	0.000011	0.087822[c]
20	0.088938 (0.087814)	0.000267 (0.000008)	0.089206 (0.087822)
40	0.089935 (0.087816)	0.000582 (0.000006)	0.090517 (0.087822)
60	0.090821 (0.087817)	0.000929 (0.000005)	0.091750 (0.087822)
80	0.091614 (0.087819)	0.001294 (0.000003)	0.092907 (0.087822)
100	0.092328 (0.087819)	0.001664 (0.000002)	0.093992 (0.087822)

[a] P(S-*b*-I) has the same composition as in Table 3. [b] χ_{comp} is again evaluated at $q = q^*$. [c] This value is again $2\chi_{cRPA}(q^*)$ at spinodals regardless of pressure. [d] χ's at the indicated pressures (>0.1 MPa) and at the corresponding T_s's are again given inside the brackets for comparison purposes.

χ_{comp}, which then enhances miscibility. In the case of σ_2 = 4.35 Å, the apparent increase of spinodal temperatures with the increase of pressure is shown. This procedure originates in the fact that χ_{comp} at the spinodals is meaninglessly small, as seen in Table 5. The increased χ_{app} due to the applied pressure impedes miscibility in the system. The spinodals in the case of σ_2 = 4.08 Å reveal the intermediate behavior. It is observed that the spinodal temperatures first decrease and then increase with pressure.[51] In this case, χ_{comp} first contributes to phase miscibility, and then χ_{app} starts to overtake χ_{comp} eventually to hinder miscibility. The calculated χ's in Table 4 clearly suggest this behavior. It is then evident that all the observed phase behavior of various UCOT block copolymer melts under pressure can be understood by the balance between χ_{app} and χ_{comp}.

Hadjuk et al. measured by using the small-angle X-ray scattering technique the pressure dependence of the order−disorder transition temperature of the P(S-*b*-I) melt with the same overall molecular weight and composition as in Figures 1 and 2.[41] At this composition, the hex morphology represents the ordered structure. It was observed that the transition temperature shows the monotonic increase by ~19 K upon ΔP = 100 MPa. In Figure 3, the theoretically predicted spinodal temperature in the case of σ_2 = 4.35 Å was also monotonically increased by ~17 K. This result implies that the compressibility difference is of little importance in the phase behavior of the P(S-*b*-I) melts, just as in that of the previously studied UCOT system, which is the P(S-*b*-BD) melts.[33,37,38] The parameter set associated with σ_2 = 4.35 Å thus turns out to be the one that is needed for the analysis of the phase behavior of the copolymer.

Landau Free Energy and Pressure Effects on Transition Temperatures

In our previous communication,[33] a Landau analysis was performed to probe compressible UCOT systems with the identical compressibility for constituent blocks. Stating briefly the Landau analysis, the free energy is expanded as a functional series in an order parameter $\bar{\psi}_1$ that represents the periodic pattern of the ordered microphase morphologies. The obtained free energy expansion is evaluated by the saddle point method only at the characteristic scattering vector q^*, at which $\det[S_{ij}^{-1}]$ exhibits a profound minimum. The absence of the compressibility difference between blocks corresponds to $\chi_{comp} \approx 0$ at $q = q^*$ in this study. The previously formulated Landau free energy associated with $\chi_{comp}(q^*) \approx 0$ can then be employed in the case of the P(S-*b*-I) melts. The final expression for the Landau free energy can be written as

$$r_T\beta\delta F = \eta[2r_T\{\chi_S(q^*) - \chi_{app}\}]\bar{\psi}_n(1)^2 - \eta a_n\bar{\psi}_n(1)^3 + \eta(b_n - \Delta)\bar{\psi}_n(1)^4 \quad (10)$$

where δF implies the difference between the free energy of the phase segregating copolymer system and that in the disordered state. The $\chi_s(q^*)$ indicates the Gaussian contribution to $\det[S_{ij}^{-1}(q^*)]$, i.e., $\eta(S_{11}° + S_{22}° + 2S_{12}°)/2D$ evaluated at $q = q^*$. The $\bar{\psi}_n(1)$ denotes the amplitude of the order parameter $\bar{\psi}_1$. The symbols a_n and b_n are the sums of all the $\vec{q}$-dependent $\Gamma^{(3)}$'s and $\Gamma^{(4)}$'s, respectively, in Leibler's Landau free energy[6] for the corresponding incompressible systems. In eq 10, Δ is given by the combination of coupled third-order and uncoupled second-order vertex functions considering the fluctuations in free volume fractions.[52] The Δ value is shown to be ignorable when chain size is big enough. The Landau free energy in eq 10 should be minimized with respect to $\bar{\psi}_n(1)$ in order to determine equilibrium microphase morphologies. As finite compressibility has been introduced into the Landau free energy, the effects of pressure on order−disorder and order−order transition temperatures can be predicted by the theory.

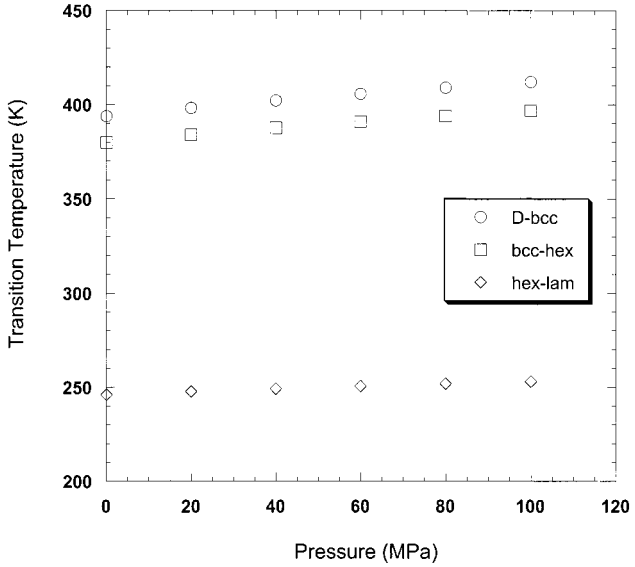

Figure 4. Various transition temperatures plotted against pressure for the P(S-*b*-I) melt with the MW's of 5100 and 15 400 for PS and PI, respectively. It is seen that the transition temperatures increase apparently linearly with pressure, which is harmonious with the behavior of spinodal temperature for the copolymer in plot c of Figure 3.

Figure 4 shows the transition temperatures for the P(S-*b*-I) melt with the same size (MW = 20 500) and composition (ϕ_{PS} = 0.257) as in Figures 1 and 2, plotted as a function of pressure up to 100 MPa. The general

trend shown in this figure is the same as the spinodals: the transition temperatures apparently increase with pressure. It was shown in our previous communication that the microphase separation behavior in typical UCOT systems, where compressibility difference between constituent blocks is insignificant, can be described using the relevant parameter $r_T\chi_{app}$ at a fixed composition.[33] The χ_{app} is proportional to $|u(\eta)|$, which is fairly linear with respect to η. As pressure is applied to the system, the density η of the system increases. Therefore, the density of the unfavorable exchange energy between the blocks accordingly increases by the function $|u(\eta)|$. This procedure then hampers miscibility eventually to reveal higher transition temperatures. The apparently linear relationship between η and $|u(\eta)|$ yields the linear increase of the transition temperatures because the relevant parameter $r_T\chi_{app}$ is fixed at a given composition.

The pressure coefficients, $\Delta T_{trs}/\Delta P$, of the transition temperatures can be extracted from Figure 4. In Figure 5, the collection of such pressure coefficients is plotted as a function of composition for the copolymers with MW = 20 500, along with the transition temperatures at 0.1 MPa. The pressure coefficients are generally higher for transitions with higher transition temperatures. Such a result stems from that the copolymer becomes more compressible at higher temperatures. Figure 6 contains the same plots as Figure 5, but for the copolymer with MW = 16 500. From the comparison of Figures 5 and 6, it is seen that the copolymers with higher molecular weights have the higher pressure coefficients of transition temperatures. This calculational result is again caused by the fact that the increase in molecular weights generally induces the increase in transition temperatures, which in turn renders the copolymer more compressible. The experimental results made by Hadjuk et al.[41] are marked in Figures 5 and 6. For the copolymer with MW = 20 500 at $\phi_{PS} = 0.257$, the order−disorder (disorder → hex) transition shows a satisfactory agreement between the experiments and the prediction. However, for the symmetric copolymer with MW = 16 500, the order−disorder (disorder → lam) transition gives a pressure coefficient of ∼18 K/100 MPa, which is far lower than our mean-field prediction of ∼29 K/100 MPa. This discrepancy is considered to result from concentration fluctuation effects, which reduce the order−disorder transition temperatures, especially around the critical point, and thus the compressibility.

For the latter symmetric copolymer, Hadjuk et al. also measured the volume change upon disordering, $\Delta V_{mix}/V$, at the transition point. It was reported by them that $\Delta V_{mix}/V = 4.5 \pm 1.5 \times 10^{-4}$ at 360 K and at 12.7 MPa.[41] The present theory can also be used to estimate $\Delta V_{mix}/V$, even though the order−disorder transition temperature in this mean-field theory is far higher than the measured one. It is shown that the theory also yields the positive volume change of $\Delta V_{mix}/V = 3.8 \times 10^{-4}$ at the same condition, which is indeed harmonious with the experimental value just given.[53]

Conclusions

A compressible RPA study for a UCOT diblock copolymer has been performed to suggest an effective Flory type interaction parameter that carries compressible nature in the system. An attempt was also made to elucidate the effects of compressibility difference between blocks on microphase separation transition behavior under pressure with such a parameter. The P(S-*b*-I) melt was chosen here as a model system.

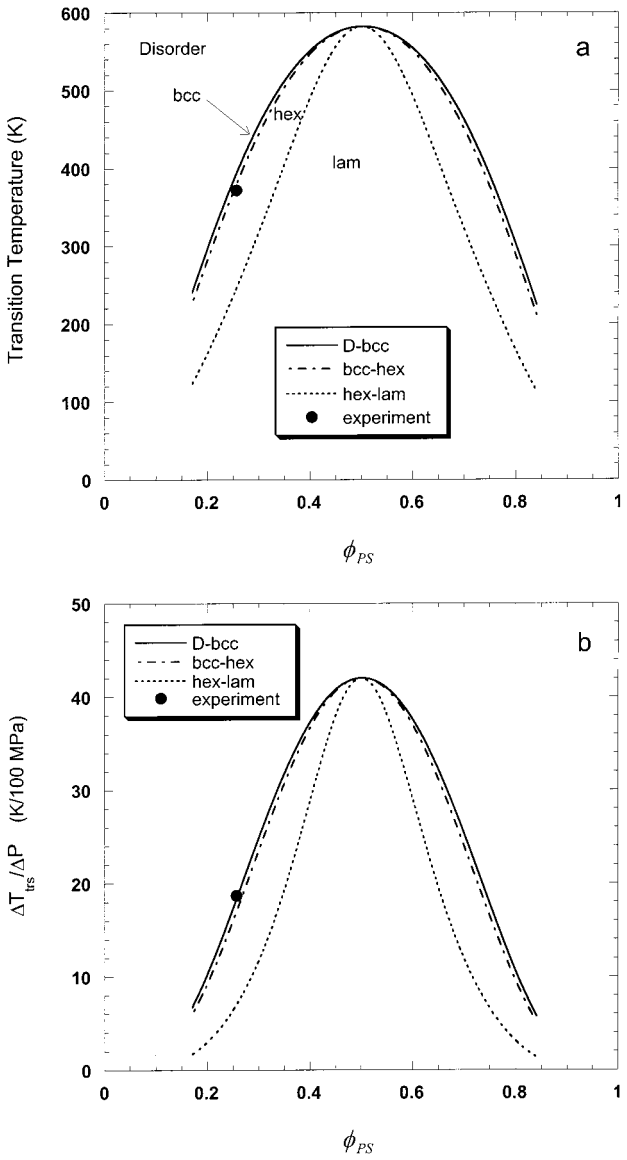

Figure 5. Collection of transition temperatures at 0.1 MPa (a) and their pressure coefficients (b) plotted as a function of ϕ_{PS} for the P(S-*b*-I) melt with the total MW = 20 500. The filled circle indicates the experimental disorder → hex transition temperature and its pressure coefficient for the same copolymer with the MW's of 5100 and 15 400 for PS and PI, respectively.

The present compressible RPA approach yielded a parameter χ_{cRPA}, which is the desired substitute for a simple Flory exchange energy in the incompressible RPA, from the analysis of the mean-field spinodals. The spinodals are characterized when the determinant, $\det[S_{ij}^{-1}]$, of the inverse correlation functions vanishes at a wavenumber $q = q^*$ that represents a certain periodic microphase structure. The χ_{cRPA} was further divided into χ_{app} and χ_{comp}. The former implies the exchange energy density ($=f_p\chi|u(\eta)|/2$), whereas the latter is a complicated function of all the molecular parameters describing each block and the Gaussian correlation functions $S_{ij}^0(q)$. It was shown that χ_{comp}, despite of its complicated form, relies on the compressibility difference between the blocks. In particular, the χ_{comp} evaluated at $q = q^*$ was found to vanish when the compressibility difference is absent. It was shown that

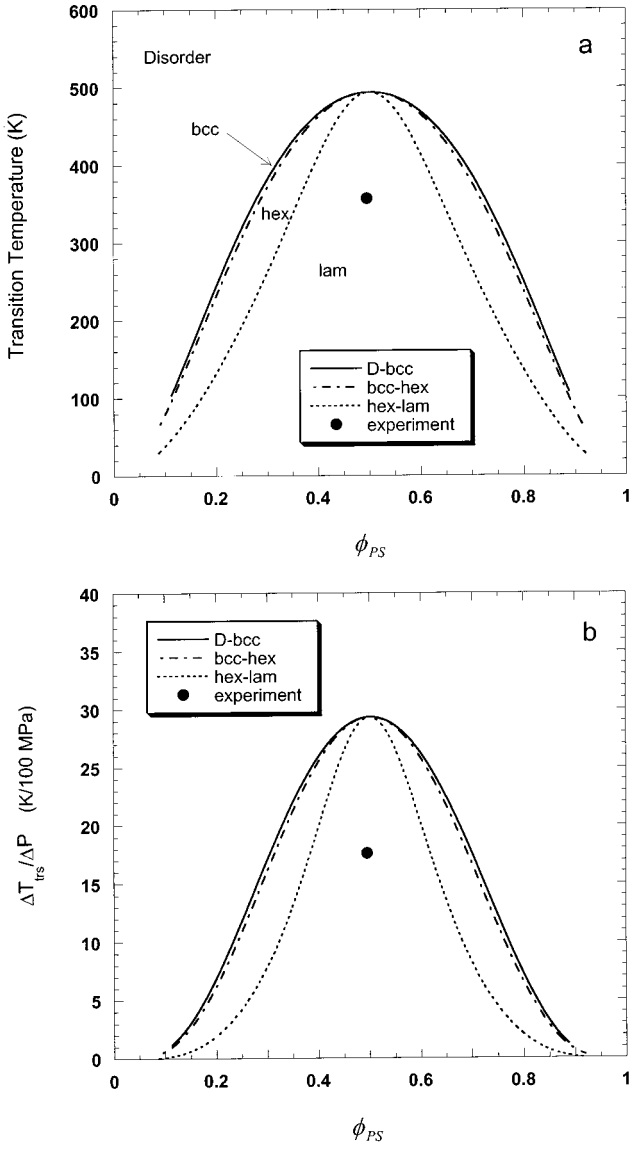

Figure 6. Collection of transition temperatures at 0.1 MPa (a) and their pressure coefficients (b) plotted as a function of ϕ_{PS} for the P(S-*b*-I) melt with the total MW = 16 500. The filled circle indicates the measured disorder → lam transition temperature and its pressure coefficient for the same copolymer that is symmetric.

χ_{app} and χ_{comp} upon pressurization contribute to phase stability in a reverse way to each other. Applied pressure suppresses the compressibility difference and thus χ_{comp}, which tends to reduce transition temperatures due to the enhanced miscibility. The exchange energy density χ_{app}, which is positive for P(S-*b*-I) and other UCOT block copolymers, increases with pressure. The increased χ_{app} tends to increase transition temperatures due to the hampered miscibility. The balance between χ_{app} and χ_{comp} was then shown to lead to all possible cases of the pressure dependence of spinodals or other transition temperatures. The linear increase in the predicted spinodals with pressure for the P(S-*b*-I) melts associated with $\chi_{comp} \approx 0$ at $q = q^*$ were shown to be harmonious with the experimental measurements obtained for the same copolymer by Hadjuk et al.; the measured order−disorder transition temperatures were also increased linearly with pressure. Such results revealed that the microphase transitions in the copolymer are mostly driven by the exchange energy density χ_{app}.

The recently formulated Landau free energy that is suitable for UCOT systems with the identical compressibility for constituents ($\chi_{comp}(q^*) \approx 0$) was applied to the P(S-*b*-I) melts. The pressure coefficients of order−disorder and order−order transition temperatures for the copolymer of two different molecular weights were calculated using the Landau free energy. When the theory is compared with the experimental measurements by Hadjuk et al. for P(S-*b*-I) with the same molecular weights, a reasonable agreement between them was reached.

Acknowledgment. This work has been supported by Korea Science and Engineering Foundation through Hyperstructured Organic Materials Research Center (HOMRC). The author acknowledges E. Cho for her assistance in numerical calculations and preparing some of the figures.

Appendix A. Cho−Sanchez Equation-of-State Model and Spinodals

In this appendix, the Cho−Sanchez (CS) equation-of-state model is briefly introduced. The CS model was originally developed for polymer blends.[30,36] A binary blend system of two polymers consists of N_1 chains of r_1-mers and N_2 chains of r_2-mers. Each polymer chain in the system is simplified to be the linear chain of tangent spherical monomers that have the identical diameter σ.

The CS model suggests the free energy as $A = A_0^{id} + A_0^{EV} + U^{nb}$. The A_0^{id} represents the ideal free energy of the noninteracting Gaussian blend system. The A_0^{EV} and U^{nb} stand for the contribution to the free energy from the excluded volume effects and the attractive interactions between nonbonded monomers, respectively. Each term of the free energy is written explicitly in the following analytical equation

$$\frac{\beta A}{rN} = \sum \frac{\phi_i}{r_i} \ln \frac{\eta \phi_i I_i \Lambda_i^{3r_i}}{r_i v^* z_i e} + \left\{ \frac{3}{2}\left[\frac{1}{(1-\eta)^2} - \left(1 - \frac{1}{r}\right)\frac{1}{1-\eta} \right] - \frac{1}{r}\left[\ln(1-\eta) + \frac{3}{2} \right] \right\} + \frac{f_p}{2}\beta\bar{\epsilon}u(\eta) \quad \text{(A1)}$$

where v^* ($= \pi\sigma^3/6$) is the volume of one monomer. In eq A1, $N = N_1 + N_2$ is the total number of chains and $r = (r_1N_1 + r_2N_2)/N$ denotes the average chain size. The ϕ_i is the close-packed volume fraction of *i*-monomers, and thus $\phi_i = r_iN_i/rN$. The Λ_i and I_i imply the thermal de Broglie wavelength of monomers on *i*-chains and the symmetry number of *i*-chains, respectively. The symbol z_i implies the conformational partition function of Gaussian *i*-chains, which will be left as an unspecified constant here. The transcendental number *e* equals 2.718 and β is $1/kT$ as usual. The η denotes the total packing density that implies the fraction of volume occupied by all the chains.

The $u(\eta)$ in eq 1 describes the packing density dependence of attractive nonbonded interactions as

$$u(\eta) = [(\gamma/C)^{p/3}\eta^{p/3} - (\gamma/C)^2\eta^2] \quad \text{(A2)}$$

where $\gamma = 1/\sqrt{2}$, $C = \pi/6$, and $p = 12$. The $u(\eta)$ in eq A2 originates in the Lennard-Jones (L-J) potential acting between two monomers. The f_p in eq A1 is a numeric

prefactor associated with the L-J potential, and is simply $f_p = 4$. The parameter $\bar{\epsilon}$, defined as $\bar{\epsilon} = \sum_{ij}\phi_i\phi_j\bar{\epsilon}_{ij}$, describes the characteristic energy of the blend, where $\bar{\epsilon}_{ij}$ implies the L-J potential depth of the attractive interactions between two monomers on i and j-chains.

To apply the free energy in eq A1 to a specific blend system, one requires various molecular parameters such as $\bar{\epsilon}_{ii}$, r_i, and σ for given homopolymers and $\bar{\epsilon}_{ij}$ for cross-interactions between different homopolymers. Homopolymer parameters can be obtained from fitting measured volumetric data to the following equation of state:

$$\eta^2\frac{\partial A}{\partial \eta} = r_T N v^* P \tag{A3}$$

The cross-interaction parameter $\bar{\epsilon}_{ij}$ is commonly estimated as $\bar{\epsilon}_{ij} = \xi(\bar{\epsilon}_{ii}\bar{\epsilon}_{jj})^{1/2}$ with an adjustable parameter ξ, which can be determined from various mixture behavior such as the following spinodal condition:

$$g_{\phi}\phi/kT = \frac{1}{r_1\phi_1} + \frac{1}{r_2\phi_2} - 2\left[\chi_{app} + \frac{v^*\kappa_T}{2\eta kT}P_{\phi}^{\,2}\right] \tag{A4}$$

where χ_{app} is already defined in eq 6 and κ_T is the isothermal compressibility. The P_ϕ describes the compressibility difference between constituents, which can be written explicitly as

$$P_{\phi}v^*/kT = \frac{f_p}{2}\{\beta\bar{\epsilon}_{11} - \beta\bar{\epsilon}_{22} - \chi(1-2\phi_1)\}\eta^2\frac{\partial u(\eta)}{\partial \eta} + \left(\frac{1}{r_1} - \frac{1}{r_2}\right)\left[\frac{3}{2}\frac{\eta^2}{(1-\eta)^2} + \frac{\eta^2}{1-\eta} + \eta\right] \tag{A5}$$

From eq A4, it can be easily seen that the compressibility term always hampers miscibility because it is always negatively contributing to spinodal condition.

Appendix B. Compressible RPA

A RPA is an approximation method to calculate the second-order monomer−monomer correlation function $G_{ij}^{(2)}$, or equivalently S_{ij}, and higher-order correlation functions $G^{(n)}$'s for the analysis of phase segregation in polymer blends and block copolymers.[5,6] Recently, the present author successfully combined the RPA with CS equation-of-state model to analyze compressibility effects.[30−33]

The basic idea of the theory follows the spirit of the incompressible RPA by Leibler.[6] A phase segregating system is characterized by the so-called order parameter ψ_i ($\equiv\langle\eta_i(\vec{r}) - \eta_i\rangle$), which is defined as the thermal average of the difference between the local density $\eta_i(\vec{r})$ and the global density η_i of i-monomers. The Landau expansion of the free energy is expressed as a series in the order parameter ψ_i, where the coefficients in the Landau expansion are called the vertex functions $\Gamma^{(n)}$. The ψ_i can also be expanded as a series in U_i, which is conjugate to the order parameter ψ_i. The coefficients appearing in the series for ψ_i are the correlation functions $G^{(n)}$'s. In estimating ψ_i, the correlation functions $G^{(n)}$ are supposed to be equal to those of noninteracting Gaussian copolymer chains, which are denoted as $G^{(n)0}$. The external potential U_i is then substituted with U_i^{eff}, which is corrected as $U_i^{eff} = U_i + W_{ij}\psi_j$ to properly take the interaction effects into account by an interaction field W_{ij}. The W_{ij} replaces the simple Flory−Huggins χ to account for the desired compressibility effects and is formulated from the CS model. The resultant self-consistent field equation is solved in an iterative technique to obtain correlation functions.[32] The correlation functions then yield the vertex functions as seen in our previous study. The second-order vertex function is only written here for example as

$$\Gamma_{ij}^{(2)} = S_{ij}^{\,-1} = S_{ij}^{\,0\,-1} + \beta W_{ij} \tag{B1}$$

It should be kept in mind that the vertex functions $\Gamma^{(n)}(\vec{q}_1, ...,\vec{q}_n)$ are nonvanishing only if $\sum_{i=1}^{n}\vec{q}_i$ vanishes.

For the analysis of compressible UCOT diblock copolymer systems, it is more convenient to use the following order parameter $\bar{\psi}_i$ instead of the original ψ_i[33]

$$\bar{\psi}_i = M_{ij}\psi_j \tag{B2}$$

where M_{ij} is defined as

$$[M_{ij}] = \begin{bmatrix} \frac{1}{2\eta} & -\frac{1}{2\eta} \\ 1 & 1 \end{bmatrix} \tag{B3}$$

The vertex functions $\Gamma^{(n)}$ in the Landau expansion of the free energy in ψ_i is then replaced with the proper vertex function $\bar{\Gamma}^{(n)}$ for $\bar{\psi}_i$ as

$$\bar{\Gamma}^{(n)}_{i_1\cdots i_n} = \Gamma^{(n)}_{j_1\cdots j_n}M_{j_1i_1}^{\;-1}\cdots M_{j_ni_n}^{\;-1} \tag{B4}$$

Here, the second-order vertex functions $\bar{\Gamma}^{(2)}$ only is written explicitly as

$$[\bar{\Gamma}_{ij}^{(2)}] = \begin{bmatrix} \eta^2(\Gamma_{11}^{(2)} - 2\Gamma_{12}^{(2)} + \Gamma_{22}^{(2)}) & \eta/2(\Gamma_{11}^{(2)} - \Gamma_{12}^{(2)}) + \eta/2(\Gamma_{12}^{(2)} - \Gamma_{22}^{(2)}) \\ \eta/2(\Gamma_{11}^{(2)} - \Gamma_{12}^{(2)}) + \eta/2(\Gamma_{12}^{(2)} - \Gamma_{22}^{(2)}) & \Gamma_{11}^{(2)}/4 + \Gamma_{12}^{(2)}/2 + \Gamma_{22}^{(2)}/4 \end{bmatrix} \tag{B5}$$

All the higher-order ones can be found from our previous communication. Among various $\bar{\Gamma}^{(n)}$'s, $\bar{\Gamma}^{(3)}_{111}$ and $\bar{\Gamma}^{(4)}_{1111}$ are of our special interest. It was shown that $\bar{\Gamma}^{(3)}_{111}$ and $\bar{\Gamma}^{(4)}_{1111}$ become identical with $\eta\Gamma_3$ and $\eta\Gamma_4$, respectively, where Γ_3 and Γ_4 are those obtained by Leibler in the incompressible RPA.[6]

The interaction field W_{ij} is obtained from the nonideal free energy, $A_0^{EV} + U^{nb}$, of the CS model. The W_{ij} then consists of the two terms L_{ij} and ϵ_{ij}^{app}, which are formulated from A_0^{EV} and U^{nb}, respectively:

$$\beta W_{ij} = L_{ij}(\eta) - \beta\epsilon_{ij}^{app}(\eta) \tag{B6}$$

where L_{ij} and ϵ_{ij}^{app} are given as

$$L_{ij}(\eta) = \frac{3}{2}\left[\frac{4}{(1-\eta)^3} + \frac{6\eta}{(1-\eta)^4} - \left(2 - \frac{1}{r_i} - \frac{1}{r_j}\right)\frac{1}{(1-\eta)^2} - \left(\eta - \frac{\eta}{r}\right)\frac{2}{(1-\eta)^3}\right] + \left(\frac{1}{r_i} + \frac{1}{r_j}\right)\frac{1}{1-\eta} + \frac{\eta}{r}\frac{1}{(1-\eta)^2} \tag{B7}$$

and

$$-\beta\epsilon_{ij}^{\mathrm{app}}(\eta) = \beta\bar{\epsilon}_{ij}f_{\mathrm{p}}\frac{u(\eta)}{\eta} + \beta(\sum_{k}\eta_k\{\bar{\epsilon}_{ik} + \bar{\epsilon}_{jk}\})f_{\mathrm{p}}\frac{\partial}{\partial\eta}\left(\frac{u(\eta)}{\eta}\right) + \frac{1}{2}\beta(\sum_{kl}\eta_k\eta_l\bar{\epsilon}_{kl})f_{\mathrm{p}}\frac{\partial^2}{\partial\eta^2}\left(\frac{u(\eta)}{\eta}\right) \quad \text{(B8)}$$

The interaction field W_{ij} given above was first derived for polymer blends with the close-packed volume fraction ϕ_i of i-monomers. The W_{ij} for polymer blends is then adopted for the corresponding block copolymers with the same ϕ_i.[30−33]

References and Notes

(1) Aggarwal, S. L. *Block Copolymers*; Plenum Press: New York, 1970.
(2) *Developments in Block Copolymers-I*; Goodman, I., Ed.; Applied Science Publishers: New York, 1982.
(3) *Thermoplastic Elastomers*; Holden, G., Legge, N. R., Quirk, R. P., Schroeder, H. E., Eds.; Hanser: New York, 1996.
(4) Hamley, I. W. *The Physics of Block Copolymers*; Oxford University Press: New York, 1998.
(5) de Gennes, P.-G. *Scaling Concepts in Polymer Physics*; Cornell University Press: Ithaca, NY, 1979.
(6) Leibler, L. *Macromolecules* **1980**, *13*, 1602.
(7) Fredrickson, G. H.; Helfand, E. *J. Chem. Phys.* **1987**, *87*, 697.
(8) Olvera de la Cruz, M. *Phys. Rev. Lett.* **1991**, *67*, 85.
(9) Olvera de la Cruz, M.; Mayes, A. M.; Swift, B. W. *Macromolecules* **1992**, *25*, 944.
(10) Milner, S. T.; Olmsted, P. D. *J. Phys. II* **1997**, *7*, 249.
(11) Podneks, V. E.; Hamley, I. W. *JETP Lett.* **1996**, *64*, 617.
(12) Podneks, V. E.; Hamley, I. W. *Pis'ma Zh. Eksp. Teor. Fiz.* **1996**, *64*, 564.
(13) Hamley, I. W.; Bates, F. *J. Chem. Phys.* **1994**, *100*, 6813.
(14) Hamley, I. W.; Podneks, V. E. *Macromolecules* **1997**, *30*, 3701.
(15) McMullen, W. E.; Freed, K. F. *Macromolecules* **1990**, *23*, 255.
(16) Dudowicz, J.; Freed, K. F. *Macromolecules* **1990**, *23*, 1519.
(17) Tang, H.; Freed, K. F. *Macromolecules* **1991**, *24*, 958.
(18) Tang, H.; Freed, K. F. *J. Chem. Phys.* **1991**, *94*, 1572.
(19) Dudowicz, J.; Freed, K. F. *J. Chem. Phys.* **1992**, *96*, 9147.
(20) Freed, K. F.; Dudowicz, J. *J. Chem. Phys.* **1992**, *97*, 2105.
(21) Dudowicz, J.; Freed, K. F. *Macromolecules* **1993**, *26*, 213.
(22) Dudowicz, J.; Freed, K. F. *Macromolecules* **1995**, *28*, 6625.
(23) Yeung, C.; Desai, R. C.; Shi, A. C.; Noolandi, J. *Phys. Rev. Lett.* **1994**, *72*, 1834.
(24) Bidkar, U. R.; Sanchez, I. C. *Macromolecules* **1995**, *28*, 3963.
(25) Hino, T.; Prausnitz, J. M. *Macromolecules* **1998**, *31*, 2636.
(26) Russell, T. P.; Karis, T. E.; Gallot, Y.; Mayes, A. M. *Nature* **1994**, *368*, 729.
(27) Karis, T. E.; Russell, T. P.; Gallot, Y.; Mayes, A. M. *Macromolecules* **1995**, *28*, 1129.
(28) Ruzette, A.-V. G.; Banerjee, P.; Mayes, A. M.; Pollard, M.; Russell, T. P.; Jerome, R.; Slawecki, T.; Hjelm, R.; Thiyagarajan, P. *Macromolecules* **1998**, *31*, 8509.
(29) Mansky, P.; Tsui, O. K. C.; Russell, T. P.; Gallot, Y. *Macromolecules* **1999**, *32*, 4832.
(30) Cho, J. *Macromolecules* **2000**, *33*, 2228.
(31) Cho, J. *Polym. Prepr.* **2000**, *41*, 1114.
(32) Cho, J. *Macromolecules* **2001**, *34*, 1001.
(33) Cho, J. *Macromolecules* **2001**, *34*, 6097.
(34) Akcasu, A. Z.; Tombakoglu, M. *Macromolecules* **1990**, *23*, 607.
(35) Akcasu, A. Z.; Klein, R.; Hammouda, B. *Macromolecules* **1993**, *22*, 1238.
(36) Cho, J.; Sanchez, I. C. *Macromolecules* **1998**, *31*, 6650.
(37) Ladynski, H.; Odorico, D.; Stamm, M. *J. Non-Cryst. Solids* **1998**, *235−237*, 491.
(38) Frielinghaus, H.; Abbas, B.; Schwahn, D.; Willner, L. *Europhys. Lett.* **1998**, *44*, 606.
(39) Frielinghaus, H.; Schwahn, D.; Mortensen, K.; Almdal, K.; Springer, T. *Macromolecules* **1996**, *29*, 3263.
(40) Schwahn, D.; Frielinghaus, H.; Mortensen, K.; Almdal, K. *Phys. Rev. Lett.* **1996**, *77*, 3153.
(41) Hajduk, D. A.; Gruner, S. M.; Erramilli, S.; Register, R. A.; Fetters, L. J. *Macromolecules* **1996**, *29*, 1473.
(42) This result implies that block copolymers phase separate only on a microscopic scale owing to the connectivity of constituent polymers.
(43) Attempts to define an effective χ parameter have been made from the compressible RPA theories.[15−24,31] Theoretical scattering intensities for compressible polymer blends and block copolymers can be formulated and then forced to conform that from de Gennes[5] or Leibler[6] in the incompressible situation. The effective χ in this approach can be shown to be dependent on the nonthermodynamic scattering lengths of the constituent monomers in the systems of interest.[24,31] In an alternative way, correlation functions or spinodals can be used as in the present study to properly define the effective χ parameter. The latter approach yields no dependence of the effective χ on the monomer scattering lengths.
(44) Quach, A.; Simha, R. *J. Appl. Phys.* **1971**, *42*, 4592.
(45) *Polymer Handbook*; Brandrup, J., Immergut, E. H., Grulke, E. A., Eds.; Wiley-Interscience: New York, 1999.
(46) Yi, Y. X.; Zoller, P. *J. Polym. Sci., Polym. Phys. Ed.* **1993**, *31*, 779.
(47) The cloud points for PS/PI blends with MW's of 2117 and 2594, respectively, were measured to yield a critical temperature $T_c \approx 388$ K. See: Rudolf, B.; Cantow, H.-J. *Macromolecules* **1995**, *28*, 6586.
(48) The χ_{comp} can be interpreted in mathematical terms. It is a common sense that the arithmetic mean of S_{11}^{-1} and S_{22}^{-1} is greater than the corresponding geometric mean: $\sqrt{S_{11}^{-1}S_{22}^{-1}} \le (S_{11}^{-1} + S_{22}^{-1})/2$. The spinodal condition yields $S_{12}^{-1} = \sqrt{S_{11}^{-1}S_{22}^{-1}}$ at q^*, which then suggests $(S_{11}^{-1} + S_{22}^{-1})/2 - S_{12}^{-1} \ge 0$ at q^*. It was shown in our previous work that $(S_{11}^{-1} + S_{22}^{-1})/2 - S_{12}^{-1}$ becomes equal to $\eta(S_{11}^{\circ} + S_{22}^{\circ} + 2S_{12}^{\circ})/2D - \chi_{\mathrm{app}}$.[33] It is seen from eqs 3 and 4 that $\eta(S_{11}^{\circ} + S_{22}^{\circ} + 2S_{12}^{\circ})/2D - \chi_{\mathrm{app}} = \chi_{\mathrm{comp}}$ at spinodals and at q^*. Therefore, it can be stated that $\chi_{\mathrm{comp}}(q^*) \ge 0$. The equality holds if $S_{11}^{-1} = S_{22}^{-1}$. It was shown that $S_{ii}^{-1}(q^*)$ strongly depends on $\bar{\epsilon}_{ii}$, and thus $S_{22}^{-1}(q^*) \to S_{11}^{-1}(q^*)$ as $\bar{\epsilon}_{22} \to \bar{\epsilon}_{11}$.[33] Consequently, we have a vanishing $\chi_{\mathrm{comp}}(q^*)$ if the compressibility difference between constituents is of little importance ($\bar{\epsilon}_{11} \approx \bar{\epsilon}_{22}$). The presence of appreciable compressibility difference ($|\bar{\epsilon}_{11} - \bar{\epsilon}_{22}| > 0$) should lead to the inequality that $\chi_{\mathrm{comp}}(q^*) > 0$. It can then be understood that χ_{comp} contains the effects of compressibility difference between the blocks.
(49) The χ_{comp} with $\sigma_2 = 4.35$ Å, if calculated at a fixed temperature (T_s at 0.1 MPa), seems to behave differently from those with the other σ_2's, as seen in Table 5. As χ_{comp} in eq 7 contains terms involving β (=$1/kT$) or β^2, appreciable increases in χ_{comp} can result from lowering temperatures. Figure 3c shows that T_s's are indeed increasing with pressure from that at 0.1 MPa. It is thus considered that those terms of χ_{comp} just mentioned come into play relatively strongly in this case.
(50) This behavior of spinodals is indeed observed in the P(EP-*b*-EE) results.[39]
(51) This complicated behavior of the calculated spinodals is harmonious with the pressure effects on the order−disorder transition temperatures of the P(EP-*b*-DMS) melts.[40]
(52) The fluctuations of free volume are described by the other order parameter ψ_2 appearing in Appendix B. It is shown in our previous communication[33] that $\psi_n(2)$, which gives the amplitude of the sinusoidal ψ_2, is on the order of $\psi_n(1)^2$.
(53) Along with the prediction of $\Delta V_{\mathrm{mix}}/V$, the present theory can also yield the enthalpy change upon disordering, ΔH_{mix} (=$\Delta U_{\mathrm{mix}} + \Delta PV_{\mathrm{mix}}$). Using the relationship that $\Delta U_{\mathrm{mix}} = RT\chi_{\mathrm{app}}\phi_1\phi_2$, ΔH_{mix} for this symmetric copolymer is predicted to be 70.8 J/mol at 0.1 MPa and 363 K. This ΔH_{mix} agrees reasonably well with the experimental value of 94.6 ± 17.2 J/mol for the same symmetric copolymer of MW = 17 700 measured by: Stuhn, B. *J. Polym. Sci.: Polym. Phys.* **1992**, *30*, 1013. Meanwhile, Kasten and Stuhn reported in a separate communication the negative volume change upon disordering of $\Delta V_{\mathrm{mix}}/V = -3 \pm 1 \times 10^{-3}$ for a slightly asymmetric P(S-*b*-I) melt with MW = 17 000. However, such a negative ΔV_{mix} should yield the decreasing transition temperatures upon pressurization due to the positive ΔH_{mix}, which is contrary to Hadjuk et al.'s scattering results. See: Kasten, H.; Stuhn, B. *Macromolecules* **1995**, *28*, 4777.

MA020059L